Cefiderocol Resistance Conferred by Plasmid-Located Ferric Citrate Transport System in KPC-Producing *Klebsiella pneumoniae*

Riccardo Polani, Alice De Francesco, Dario Tomolillo, Irene Artuso, Michele Equestre, Rita Trirocco, Gabriele Arcari, Guido Antonelli, Laura Villa, Gianni Prosseda, Paolo Visca, Alessandra Carattoli

Cefiderocol (FDC), a siderophore-cephalosporin conjugate, is the newest option for treating infection with carbapenem-resistant gram-negative bacteria. We identified a novel mechanism contributing to decreased FDC susceptibility in *Klebsiella pneumoniae* clinical isolates. The mechanism involves 2 coresident plasmids: pKpQIL, carrying variants of bla_{KPC} carbapenemase gene, and pKPN, carrying the ferric citrate transport (FEC) system. We observed increasing FDC MICs in an *Escherichia coli* model system carrying different natural pKpQIL plasmids, encoding different

K. pneumoniae carbapenemase (KPC) variants, in combination with a conjugative low copy number vector carrying the *fec* gene cluster from pKPN. We observed transcriptional repression of *fiu*, *cirA*, *fepA*, and *fhuA* siderophore receptor genes in bla_{KPC}–*fec*–*E. coli* cells treated with ferric citrate. Screening of 27,793 *K. pneumoniae* whole-genome sequences revealed that the *fec* cluster occurs frequently in some globally distributed different KPC–producing *K. pneumoniae* clones (sequence types 258, 14, 45, and 512), contributing to reduced FDC susceptibility.

*K*lebsiella pneumoniae is 1 of 6 global leading ESKAPE pathogens (*Enterococcus faecium*, *Staphylococcus aureus*, *K. pneumoniae*, *Acinetobacter baumannii*, *Pseudomonas aeruginosa*, and *Enterobacter* spp.) associated with high morbidity and mortality rates and antimicrobial resistance (*1*). Among those pathogens, the World Health Organization designated carbapenem-resistant *K. pneumoniae* as a priority pathogen (*2*). In 1996, *K. pneumoniae* carbapenemase (KPC) was identified in *K. pneumoniae* sequence type (ST) 258 in the United States and then spread worldwide (*3–5*). To date, bla_{KPC} gene variants have been found on different plasmid types; pKpQIL is prevalent in successful clones ST258 and ST512 (*6,7*).

Author affiliations: Sapienza University of Rome, Rome, Italy
(R. Polani, A. De Francesco, D. Tomolillo, R. Trirocco, G. Arcari,
G. Antonelli, G. Prosseda, A. Carattoli); University of Pavia, Pavia,
Italy (D. Tomolillo); Istituto Superiore di Sanità, Rome (I. Artuso,
M. Equestre, L. Villa); University of Insubria, Varese, Italy
(G. Arcari); Sapienza University Hospital "Policlinico Umberto I,"
Rome (G. Antonelli); Roma Tre University, Rome (P. Visca)

Since 2015, ceftazidime/avibactam (CZA) has been available for treatment of complicated and deepseated infections, including bacteremia caused by carbapenemase-producing Enterobacterales in adults (*8*). CZA combines ceftazidime, a third-generation cephalosporin, and avibactam, a β-lactamase inhibitor (*9*). Since 2018, KPC-producing CZA-resistant *K. pneumoniae* strains have been described (*10,11*) carrying mutations in the Ω-loop of the KPC protein, such as KPC-31 (*12,13*).

Cefiderocol (FDC), approved by the US Food and Drug Administration in 2020, is available to treat Enterobacterales, *Acinetobacter baumannii*, and *Pseudomonas aeruginosa* invasive infections caused by carbapenem- and CZA-resistant strains (https://www.accessdata.fda.gov/drugsatfda_docs/nda/2020/209445Orig1s002.pdf). FDC is a cephalosporin linked with a chlorocatechol group, which provides the drug with a siderophore-like moiety that serves as a Trojan horse to gain access to the bacterial periplasm. The chlorocatechol group is thought to enhance the entry of FDC in the bacterial cell through energy-dependent uptake

by chromosome-encoded ferric siderophore transporters (*14,15*). To determine the mechanism of FDC resistance in KPC-producing *K. pneumoniae*, we analyzed the contribution of a plasmid-encoded ferric citrate uptake system (FEC), which acts synergistically with CZA-resistant KPC variants.

Materials and Methods

K. pneumoniae Isolates

K. pneumoniae strains PL1, PL2, PL3, and PL4 were isolated at the University Hospital Policlinico Umberto I, Rome, Italy, from blood samples of 1 patient during 1 month of hospitalization. The strains were processed for routine diagnostics and compared with 31 previously described strains (Appendix 1 Table 1, https://wwwnc.cdc.gov/EID/article/31/1/24-1426-App1.pdf).

FDC Antimicrobial Susceptibility

We determined FDC MICs by using ComASP (Liofilchem, https://www.liofilchem.com) or by using a ComASP panel enriching iron-depleted cation-adjusted Mueller-Hinton broth with 0.5 µM or 5.0 µM ammonium ferric citrate or trisodium citrate dihydrate (Merck KGaA, https://www.emdgroup.com). We preliminarily determined the citrate concentration used for induction of the FEC system in the *E. coli* model, and 0.5 µM ammonium ferric citrate was the minimal concentration that did not increase the FDC MIC by >1-fold in treated compared with untreated *E. coli* strains.

Whole-Genome Sequencing

We purified genomic DNA by using the MagaBio Bacterium DNA Purification Kit III (Hangzhou Bioer Technology Co., https://www.bioer.com) and GenePure Pro Nucleic Acid Purification System (Bioer Technology, https://www.bioer.com.cn), and we used NanoDrop One Microvolume UV-Vis Spectrophotometer and Qubit 4.0 Fluorometer (Invitrogen, https://www.thermofisher.com) to assess. We prepared DNA libraries by using the Nextera XT DNA Library Preparation Kit and loaded them onto a MiSeq Reagent Kit v.3 cartridge (Illumina, https://www.illumina.com). We performed paired-end sequencing on an Illumina MiSeq platform, with a read length of 2 × 300 bp. We trimmed resulting reads by using trimmomatic (*16*) and assembled them by using SPAdes (*17*).

Long-Reads Sequencing

We performed Oxford Nanopore Technologies (ONT) sequencing on a MinION Mk1C sequencing platform (https://nanoporetech.com). We extracted genomic DNA by using a Monarch HMW DNA Extraction Kit for Tissue (NEB, https://www.neb.com) and prepared libraries by using ONT Rapid Barcoding Kit 24 and sequencing on R10.4.1 flow cells. We performed long-read assemblies by using Flye (*18*).

We analyzed hybrid assembly obtained by Unicycler (*19*) and Hybracter (*20*) by using Staramr (https://bio.tools/staramr). We annotated genomes by using Prokka (*21*) and identified single-nucleotide polymorphisms by using Snippy (https://github.com/tseemann/snippy).

pKpQIL Plasmid Transformation

We introduced plasmid DNA extracted by using a Pureyield Plasmid Midiprep System (Promega, https://www.promega.com) in chemically competent *E. coli* Max efficiency DH5-α cells (Thermo Fisher Scientific, https://www.thermofisher.com). We selected transformants on Luria broth (LB) agar plates containing ceftazidime (6 mg/L).

R69c and R69c-FEC Plasmid Assembly

We obtained the R69c vector (GenBank accession no. PQ130559) by cloning the chloramphenicol resistance *catA* gene amplified from Addgene plasmid #46569 in the *Sma*I site of R69#1 (European patent EP3541942B1, A. Carattoli, A. Endimiani, https://patents.google.com/patent/EP3541942B1/de?oq=EP3541942B1, accessed November 29, 2024). We obtained PCR products by using PCRBIO VeriFi Polymerase (PCR Biosystems, https://pcrbio.com) and primers listed in Appendix 1 Table 2.

We obtained the R69c-FEC vector (GenBank accession no. PQ085644) by cloning the 7,993-bp *fec* PCR product (Appendix 1 Figure 1) from the PL3 strain and cloned it in R69c PmeI site. Both clonings were performed by using GeneArt Gibson Assembly HiFi Master Mix (Thermo Fisher Scientific).

We extracted plasmids by using ZymoPURE II Plasmid Maxiprep Kit (Zymo Research, https://www.zymoresearch.com) concentrated by Microcon DNA Fast Flow device (Merck KGaA). We performed transformations by using MAX Efficiency DH5α-T1R Competent Cells (Thermo Fisher Scientific) selected on chloramphenicol 25 mg/L LB agar plates.

Plasmid Conjugation

We grew donor and recipient strains separately in LB broth without antibiotics at an optical density of 1 McFarland. We pooled 50 µL of each culture and dropped 20 µL of the mixture on an LB plate without antibiotics and incubated it at 37°C for 6–10 hours. A patina from

the conjugation spot was diluted and plated on LB agar plates containing 25 mg/L chloramphenicol and 6 mg/L CAZ. We sequenced selected positive exconjugants by using Illumina and ONT procedures.

RNA Isolation and Quantitative Reverse Transcription PCR

We conducted bacterial RNA purification on R69c/R69c-FEC-PL3 exconjugant pairs grown in liquid iron-depleted media in the presence of 0 μM, 0.5 μM, or 5.0 μM ammonium ferric citrate by using a hot phenol extraction method (*22*). We conducted cDNA synthesis and quantitative reverse transcription PCR analyses on a 7300 real-time PCR system (Applied Biosystems, https://www.thermofisher.com) (*23*). We obtained cDNA for *nusA* (used as normalizer), *fiu*, *cirA*, *fepA*, *fhuA*, or *fecA* genes (Appendix 1 Table 2).

Global Distribution of *fec* Gene Cluster

As of July 4, 2024, we downloaded 27,993 *K. pneumoniae* genomes from the Pasteur Institute BIGSdb *Klebsiella pneumoniae* database (https://bigsdb.pasteur.fr) together with their metadata (Appendix 2 Table, https://wwwnc.cdc.gov/EID/article/31/1/24-1426-App2.xlsx). We included 35 strains from our study and previous studies in the collection (Appendix 1 Table 1).

We screened *K. pneumoniae* genomes for the *fec* operon by using the BLASTN tool in the Bacterial Isolate Genome Sequence BIGSdb database (https://bigsdb.pasteur.fr). We used as reference the *fecABCDE* operon and *fecIR* regulatory genes from *K. pneumoniae* PL3 (GenBank accession no. CP168103, nt positions 113339–121331). The *fec* gene cluster was considered present if the E-value was <1e^{-10} and identity was >85% across ≥90% of the sequence length.

We assessed the presence of the FIB(K) replicon (GenBank accession no. JN233704) by using the BLASTN tool. We also determined the presence of bla_{VIM}, bla_{NDM}, and bla_{KPC} genes by using the gene presence tool at the Pasteur Institute website (https://bigsdb.pasteur.fr) with minimum percentage identity of 95% and a minimum percentage alignment of 99%.

Phylogenetic Analysis

We used the Prokka tool (*20*) to annotate 2,493 genomes belonging to ST101, ST307, and ST512 (Appendix 3 Table, https://wwwnc.cdc.gov/EID/article/31/1/24-1426-App3.xlsx). We used Roary (*24*) to generate core-genome alignments, using MAFFT (*25*), accordingly, to the ST and IQ-TREE 2 (*26*) to construct phylogenetic trees with 1,000 ultrafast bootstrap iterations.

Results

Effect of KPC Variants on Reduced Susceptibility to FDC

Our initial aim with this study was to explain the different levels of FDC resistance in 4 ST512 *K. pneumoniae* clinical isolates (PL1, PL2, PL3, and PL4) from 1 patient during 1 month of hospitalization. PL3 was resistant to FDC (MIC 4 mg/L), whereas FDC MICs PL1, PL2, and PL4 were below the breakpoint value (0.5–2.0 mg/L; Appendix 1 Table 1). The PL1–4 genomes were closely related at the chromosomal level (6–22 single-nucleotide polymorphisms and indels on the chromosome; Appendix 4 Table, https://wwwnc.cdc.gov/EID/article/31/1/24-1426-App4.xlsx) but showed different bla_{KPC} genes and plasmid content. All PL1–4 *K. pneumoniae* strains carried different pKpQIL variants plus an IncX3 plasmid and a small ColR-NAI plasmid. The pKpQIL-PL1 plasmid harbored 2 copies of the bla_{KPC-3} gene, both pKpQIL-PL2 and pKpQIL-PL4 carried 1 copy of bla_{KPC-3} and 1 copy of bla_{KPC-31}, whereas pKpQIL-PL3 carried 2 copies of bla_{KPC-31} (Appendix 1 Figure 2). Isolates PL2 and PL3 were also enriched with the pKPN plasmid, which was absent in PL1 and PL4. In PL2, pKPN was fused with pKpQIL-PL2 in the $tnpR$-FIIK$_1$ integration site, forming a 263,486-bp plasmid. The hybrid pKPN-pKpQIL-PL2 plasmid was not transferable by transformation or conjugation and could not be further studied. In PL3, the stand-alone pKPN plasmid had acquired the *fec* gene cluster encoding for a FEC system. The *fec* gene cluster was unique to the pKPN plasmid in PL3 and was absent in PL1, PL2, and PL4. The *fec* genes mapped (alongside an ABC glutathione transporter, the *lacZ*, *lacY*, and *lacI* genes) between 2 IS*4321* elements positioned between the *tnpR* gene and the FIIK replicon (Appendix 1 Figure 3).

Acquisition of *fec* genes was suspected to correlate with increased FDC MICs of PL3. We then measured FDC MICs for all KPC-producing *K. pneumoniae* clinical strains in our collection isolated since 2018 with a completely sequenced genome, in search for *fec*, other siderophore receptors, and porin gene sequences in their genomes (Appendix 1 Table 1).

FDC MICs were 0.25–32 mg/L. The lowest (0.25 mg/L) was measured in a strain producing KPC-3 (strain 3), encoding the yersiniabactin siderophore-dependent iron uptake system, the wild-type CirA and Fiu siderophore receptors, and a wild-type OmpK36 porin (*27*). The highest FDC MIC (32 mg/L) was for a strain producing VIM (Verona
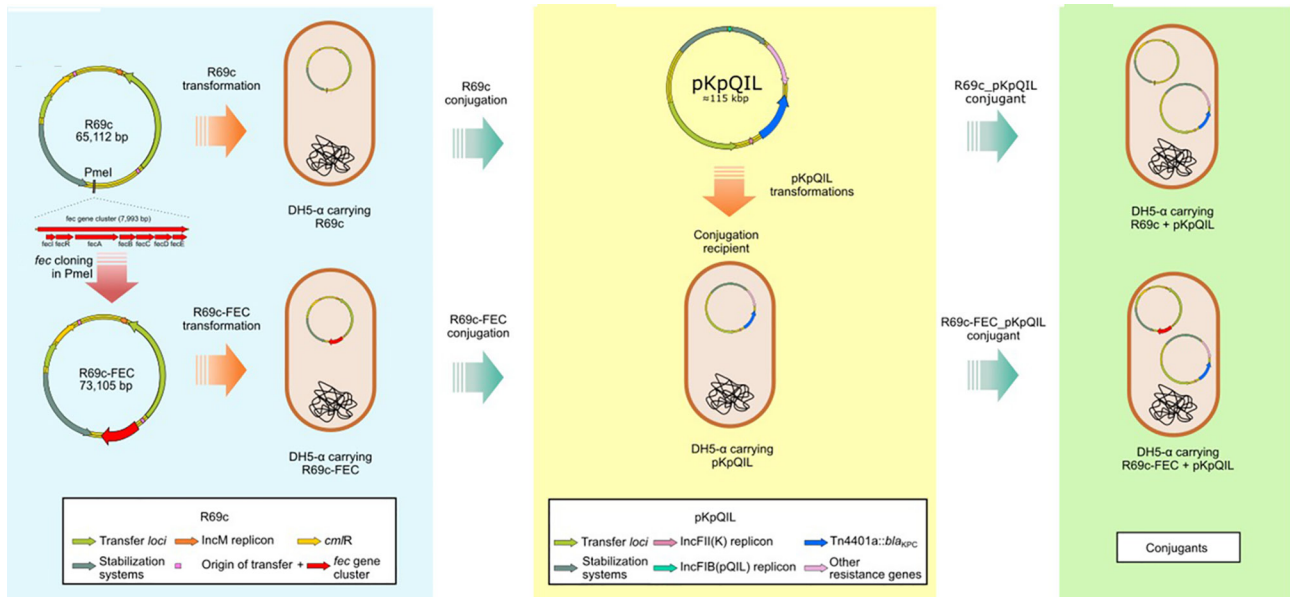
Figure 1. Schematic representation of R69c and R69c-FEC conjugation in *Escherichia coli* DH5-α recipient carrying the pKpQIL plasmids R69c and R69c-FEC and pKpQIL major features in study of cefiderocol resistance conferred by plasmid-located ferric citrate transport system in KPC–producing *Klebsiella pneumoniae*. The left panel (blue) represents construction of the R69c and R69c-FEC donor vectors, both introduced by transformation in *E. coli* DH5-α chemically competent cells. The central panel (yellow) shows the pKpQIL transformation of *E. coli* DH5-α chemically competent cells with different pKpQIL natural plasmids extracted from *K. pneumoniae* strains. The right panel (green) represents the exconjugant pairs obtained by conjugation of the R69c vectors into the recipients carrying the different pKpQIL plasmids. FEC, ferric citrate transport system; KPC, *Klebsiella pneumoniae* carbapenemase.

integron-encoded metallo-β-lactamase) and KPC carbapenemases (strain 0296), characterized by a nonsense mutation in the gene encoding the siderophore receptor CirA (E133X) (*28*).

Presence of CZA-resistant variant KPC-31, KPC-70, or KPC-68 was associated with high MICs (4 mg/L). Higher MICs (1–2 mg/L) for FDC were obtained in *E. coli* Top-10 transformed with the $bla_{\text{KPC-31}}$,

$bla_{\text{KPC-70}}$, or $bla_{\text{KPC-68}}$ genes, respectively cloned in the pTopo-KanR vector (Appendix 1 Table 1).

In addition to the role of KPC variants in determining FDC resistance levels, we noticed that *K. pneumoniae* exhibiting higher FDC MICs were positive for the FEC system (*29*), carried by the pKPN plasmid (*30*). The *fec* gene cluster was identified in 13/35 isolates from the collection. Eleven
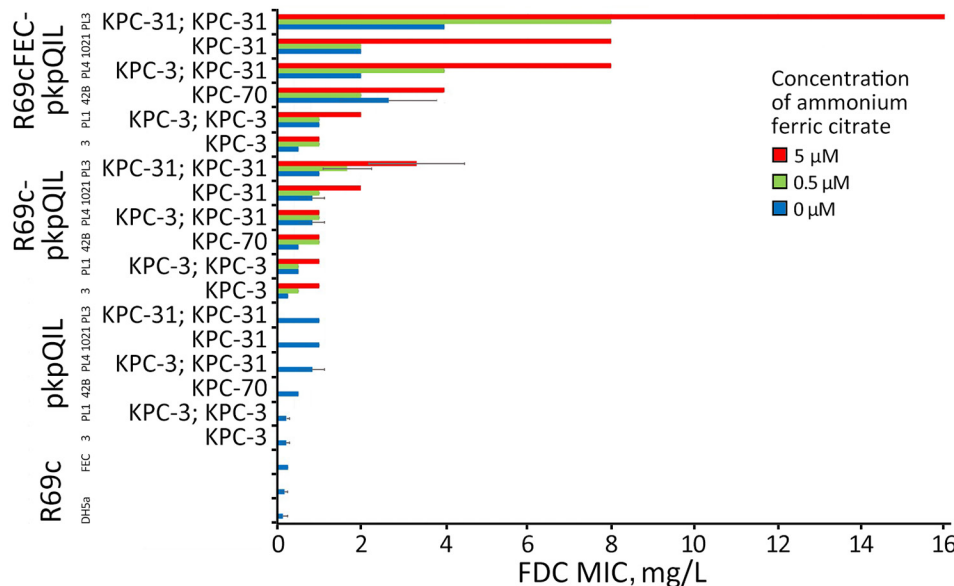

Figure 2. FDC MICs of KPC-producing *Escherichia coli* in a study of cefiderocol resistance conferred by plasmid-located ferric citrate transport system in KPC-producing *Klebsiella pneumoniae*. FDC susceptibility tests were performed according to manufacturer directives, with concentrations of 0 µM, 0.5 µM, and 5 µM ammonium ferric citrate on *Escherichia coli* DH5-α cells carrying different combinations of pKpQIL, R69c, and R69c-FEC plasmids. FDC, cefiderocol; KPC, *Klebsiella pneumoniae* carbapenemase.
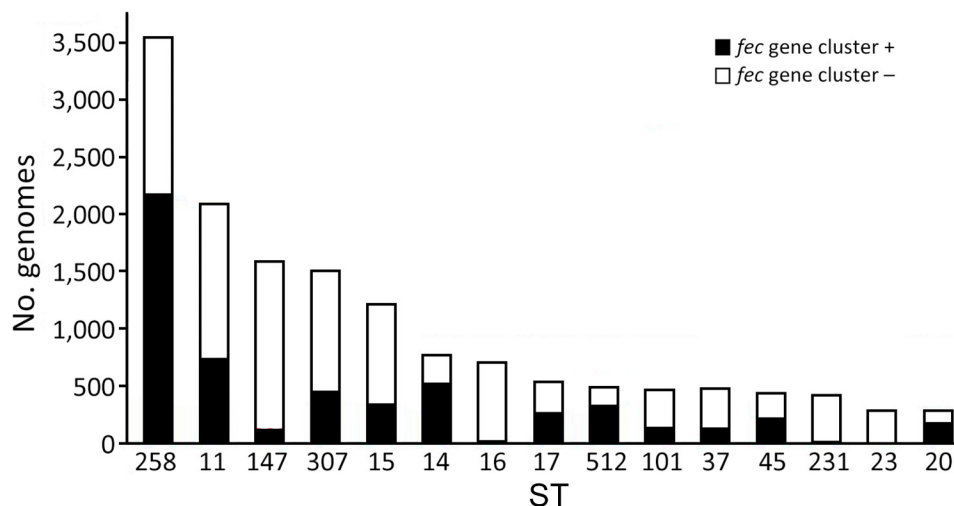
KPC-31–producing strains belonging to different STs showed FDC MICs of 1–2 mg/L, but 2 KPC-31 strains carrying the *fec* gene cluster reached a MIC of 4.0 mg/L (Appendix 1 Table 1). We hypothesized that the plasmid-borne FEC system could reduce the susceptibility to FDC in *K. pneumoniae* clinical isolates.

E. coli Model

We constructed an in vitro model in isogenic *E. coli* DH5-α cells, suitable for studying the effect of the FEC transport system on FDC resistance levels, excluding the contribution of other resistance factors, siderophore receptors, and porins encoded by the *K. pneumoniae* clinical isolates. The model consisted of the 2-step introduction in *E. coli* DH5-α cell of pKpQIL plasmids carrying different KPC variants and an engineered 64-Kb R69c self-conjugative plasmid vector carrying the *K. pneumoniae fec* gene cluster.

First, selected pKpQIL plasmid variants were individually introduced by transformation into chemically competent *E. coli* DH5-α cells. We tested the model on pKpQIL transformants obtained from strains 3, 42B, and 1021, encoding the KPC-3, KPC-70, and KPC-31 variants, respectively (Appendix 1 Table

Figure 3. Expression analysis of siderophore receptor genes in the presence and absence of plasmidic *fec* gene cluster and ferric citric inducer in an *Escherichia coli* model used in a study of cefiderocol resistance conferred by plasmid-located ferric citrate transport system KPC-producing *Klebsiella pneumoniae.* A) Transcription of the *fecA* genes in the DH5-α strain carrying R69c or R69c-FEC, determined by using primer pairs able to discern the chromosomal *fecA* allele from the *K. pneumoniae fecA* gene in the *fecABCDE* operon or a primer pair recognizing both chromosomal and plasmidic *fecA* alleles (Appendix 1 Table 2, https://wwwnc.cdc.gov/EID/article/31/1/24-1426-App1.pdf). The relative quantitative analysis of the transcripts was based on the $2^{-\Delta\Delta CT}$ method (*31*). In both bar graphs, the relative values were calculated with respect to the transcript level observed in the R69c carrying strains and set to 1. B) Transcription of the siderophore receptor genes *fiu*, *cirA*, *fepA*, and *fhuA* in the R69c-FEC and R69c strains grown in the absence of ferric citrate or in the presence of 0.5 µM or 5.0 µM ferric citrate, relative to the R69c strain grown without ferric citrate, which is set to 1. The relative quantitative analysis of the transcripts was based on the $2^{-\Delta\Delta CT}$ method (*31*). Error bars represent SDs. Statistical significance was determined by using a paired 2-tailed Student *t*-test comparing the dataset obtained from the 2 strains grown under the same conditions. FEC, ferric citrate transport system; KPC, *Klebsiella pneumoniae* carbapenemase.

Figure 4. Distribution of the *fec* gene cluster among prevalent STs of *Klebsiella pneumoniae*. Distribution of the *fec* gene cluster, represented by a black bar (number of positive genomes) or a white bar (number of negative genomes), across the total analyzed genomes for prevalent STs in the *K. pneumoniae* database (Appendix 3 Table, https://wwwnc.cdc.gov/EID/article/31/1/24-1426-App3.xlsx). ST, sequence type.

3). We also studied pKpQIL transformants carrying copies of the bla_{KPC} gene obtained from *K. pneumoniae* PL1, PL3, and PL4 strains.

Second, the 64-Kb R69c, self-conjugative plasmid vector was engineered to host *fec* genes. The R69c vector is a derivative of the R69 IncM natural plasmid (GenBank accession no. KM406488) and carries the *catA* gene, conferring chloramphenicol resistance. R69c is a self-conjugative, low-copy-number plasmid that simulates the horizontal transmission of the pKPN natural plasmid. It carries all the genes enabling conjugation at high efficiency ($1×10^{-2}$ conjugants/recipient cell), conferring stabilization, and the IncM replicon for replication and copy number control (Appendix 1 Figure 1). The plasmid enables cloning and transfer of genetic determinants at low copy numbers by conjugation. Because R69c contains a stabilization system, after chloramphenicol selection of transconjugants, the recipient *E. coli* clones do not need further antimicrobial selection to ensure plasmid maintenance. The *fecIR-fecABCDE* gene cluster, including the Fur and iron-regulated promoter regions (*32,33*) (Appendix 1 Figure 4), were amplified from the pKPN-PL3 *K. pneumoniae* plasmid. The resulting PCR product of 7,993 bp, consisting of the *fecIR* promoter region, the *fecI* and *fecR* regulatory genes, and the *fecA*, *fecB*, *fecC*, *fecD*, and *fecE* genes encoding the complete FEC system with internal regulatory regions, was cloned in the unique PmeI restriction site of R69c, obtaining the 73 Kb vector, named R69c-FEC (Appendix 1 Figure 1).

Evaluation of FDC MICs in the *E. coli* Model

We introduced R69c and R69c-FEC vectors by conjugation in DH5-α pKpQIL transformants (Appendix 1 Table 3) by obtaining pairs of exconjugants carrying the same pKpQIL variant and, alternatively, the R69c vector with or without the cloned *fec* gene cluster (Figure 1). As an *E. coli* K-12 derivative, strain DH5-α cells possess the chromosomal *fec* gene cluster (94.51% nt identity, 96% coverage; Appendix 1 Figure 4). Higher FDC MICs were invariably observed for exconjugants carrying the R69c-FEC, relative to the isogenic strain carrying the same pKpQIL with R69c lacking the *fec* gene cluster (Figure 2). The highest FDC MIC of 4 mg/L in iron-depleted media was obtained for the exconjugant carrying both pKpQIL-PL3 and R69c-FEC. The respective comparative exconjugant carrying the R69c reached an FDC MIC of 1 mg/L.

We tested in vitro susceptibility to FDC of R69c and R69c-FEC exconjugant pairs under inducing conditions by adding ferric citrate, which serves as substrate and inducer of the FEC system. In our experimental conditions, 0.5 μM or 5.0 μM of ferric citrate increased the FDC MICs of R69c/R69c-FEC DH5-α cells relative to untreated cells. The effect in strains carrying the R69c vector without the cloned *fec* gene cluster was attributed to the chromosomal *fec* gene cluster in the DH5-α background. We did not observe increased FDC MICs when using 0 μM, 0.5 μM, and 5.0 μM trisodium citrate dihydrate without iron (data not shown). The highest FDC MICs were reached by R69c-FEC-PL3 (MICs 8 in the presence of 0.5 μM and 16 mg/L in the presence of 5.0 μM ferric citrate). Under the same conditions, R69c-PL3 FDC MICs were 2 and 4 mg/L (Figure 2; Appendix 1 Table 3). The experiments performed with R69c-FEC/R69c-1021, R69c-FEC/R69c-42B, and R69c-FEC/R69c-PL4 pairs (Appendix 1 Table 3) demonstrated that the presence of an inhibitor-resistant KPC variant, such as KPC-31

and KPC-70 in combination with the plasmid-located *fec* gene cluster was sufficient to reduce FDC susceptibility (MIC ≥2.0 mg/L) relative to the R69c controls lacking the *fec* gene cluster. Further FDC MIC increment can be obtained by treatment with ferric citrate (MIC≥4.0 mg/L).

Because the FEC system is implicated in iron delivery to the cell, we compared the mRNA transcription of *fiu*, *cirA*, *fepA*, and *fhuA* siderophore receptor genes and the endogenous *fec* gene cluster in DH5-α carrying the R69c-FEC plasmid with DH5-α carrying the R69c, both in the presence or absence of ferric citrate. The expression of the R69c-located *fecA* cluster was estimated to be 3-fold higher than that of the chromosomal DH5-α *fec* cluster (Figure 3, panel A).

We observed a substantial reduction of the expression of *fiu*, *cirA*, *fepA*, and *fhuA* siderophore receptor genes growing the cells in the presence of 0.5 µM and 5.0 µM ferric citrate (relative to no fer-

ric citrate). The inhibition of *fiu*, *cirA*, *fepA*, and *fhuA* gene expression was almost complete (90%) in cells carrying the R69c-FEC plasmid and only partial in R69c-carrying cells (30%–40%, R69c-FEC vs. R69c; Figure 3, panel B). The markedly reduced expression of ferrisiderophore receptor genes caused by the cloned *K. pneumoniae fec* gene cluster correlated with the higher FDC MICs observed in R69c-FEC-positive strains in those conditions.

Prevalence of FEC Siderophore Transport System in *K. pneumoniae*

We performed global screening of the *fec* gene cluster in 27,793 *K. pneumoniae* whole-genome sequences downloaded from the Pasteur Institute database (https://bigsdb.pasteur.fr/klebsiella; Appendix 2 Table). The resulting dataset included genomes of globally prevalent clones (Figure 4).

The *fec* gene cluster was detected in 10,672 isolates across the dataset (38.4%), of which 2,658 (24.0%)
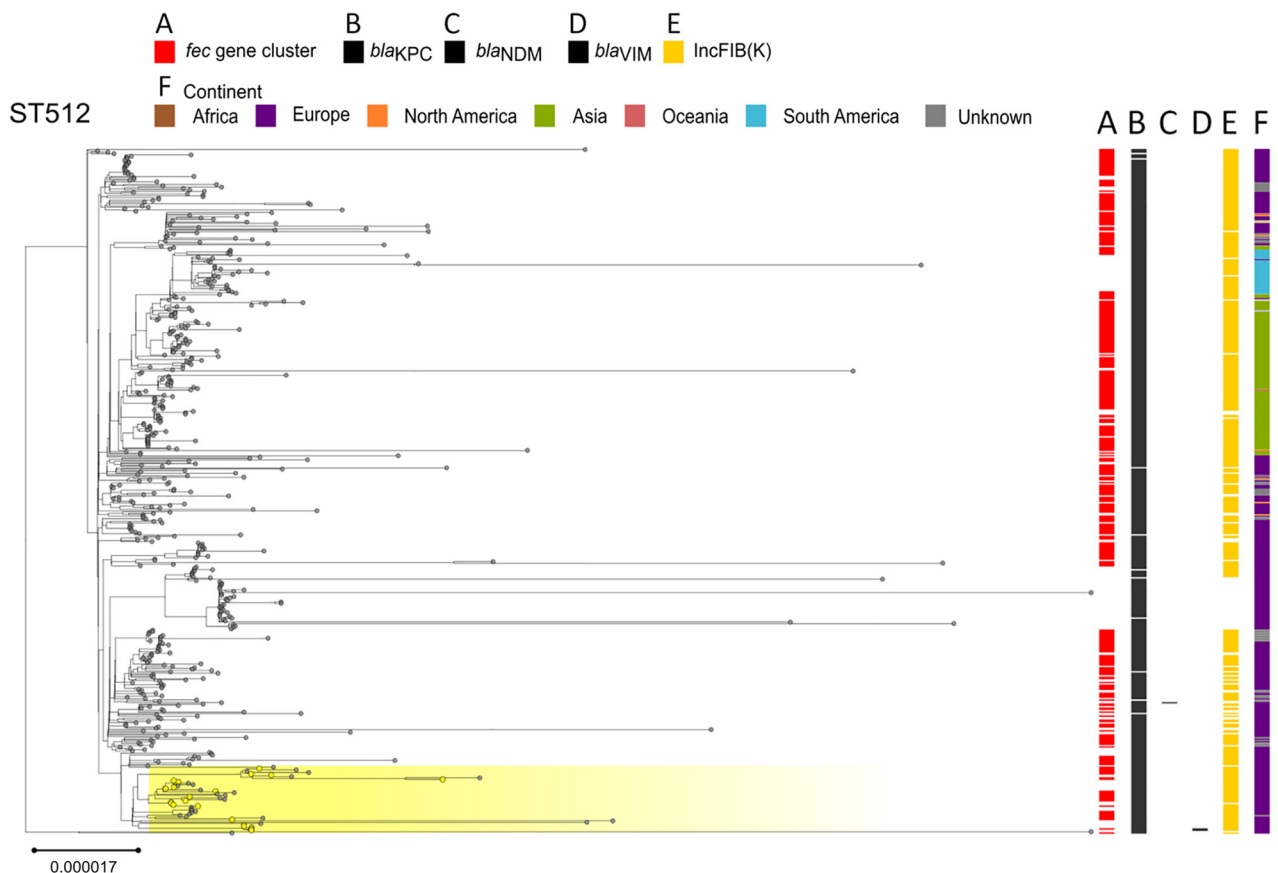
Figure 5. Phylogenetic analysis of *Klebsiella pneumoniae* ST512 based on core-genome alignment of 510 *K. pneumoniae* ST512 isolates. The tree is midpoint rooted, and the scale bar represents the number of substitutions per site. The presence of the *fec* operon is indicated in red; *bla*KPC, *bla*VIM, and *bla*NDM genes in black; and the FIB(K) replicon in orange. Yellow shading indicates genomes sequenced in this study or our previous studies (Appendix 1 Table 1, https://wwwnc.cdc.gov/EID/article/31/1/24-1426-App1.pdf). The best-fit model was selected by ModelFinder (http://www.iqtree.org/ModelFinder). Thhttp:e tree was visualized with Microreact (https://microreact.org) and adjusted by using the InkScape software (https://www.inkscape.org). ST, sequence type.
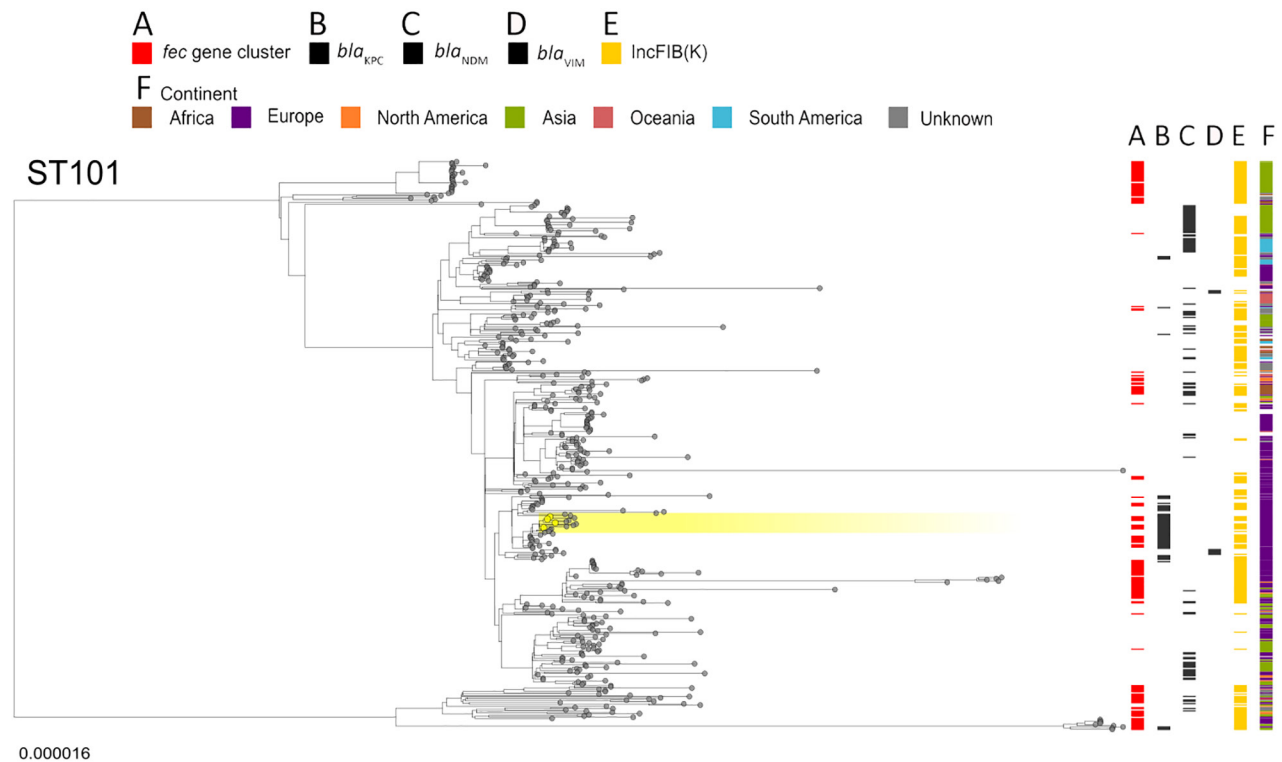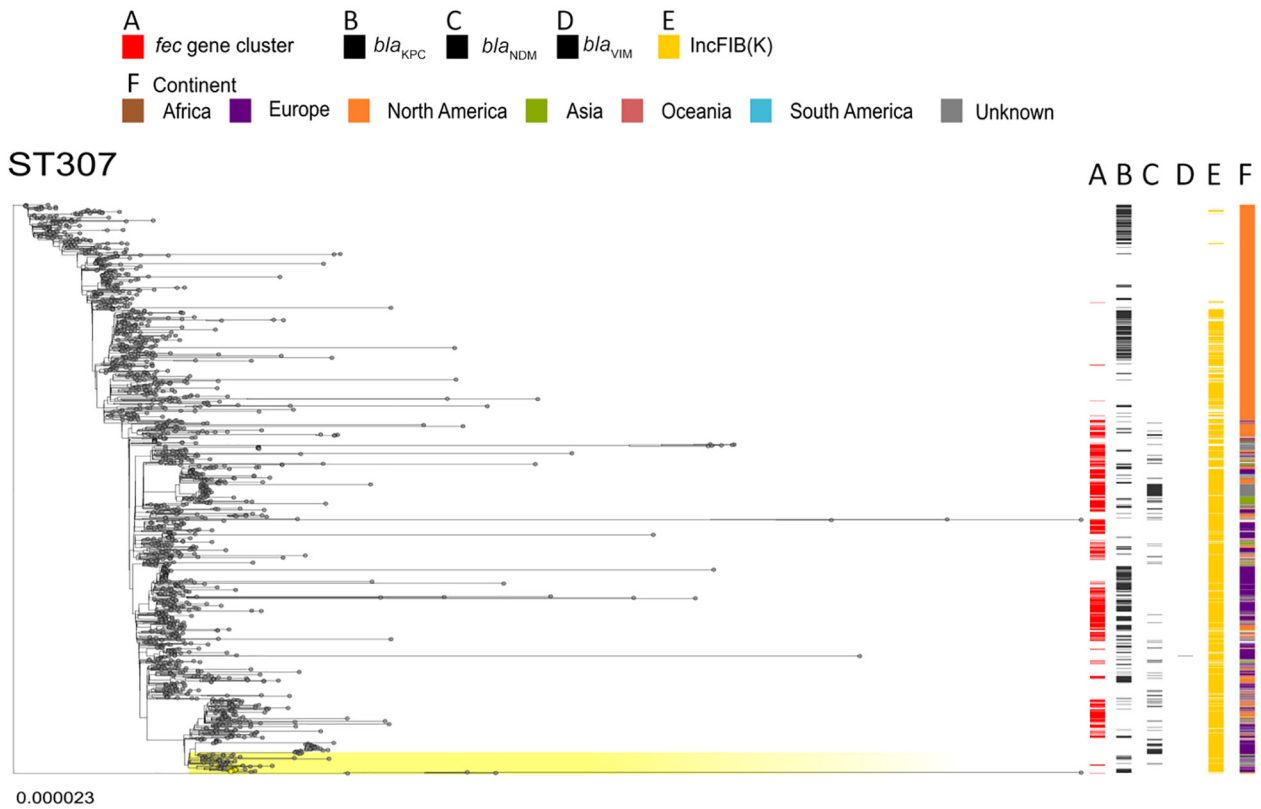
Figure 6. Phylogenetic analysis based on core-genome alignments of 468 *Klebsiella pneumoniae* ST101 isolates in a study of cefiderocol resistance conferred by plasmid-located ferric citrate transport system in *K. pneumoniae* carbapenemase–producing *K. pneumoniae*. The trees are midpoint rooted, and the scale bar represents the number of substitutions per site. The presence of the *fec* operon is indicated in red; bla_{KPC}, bla_{VIM}, and bla_{NDM} genes in black; and the FIB(K) replicon in orange. Yellow shading indicates genomes sequenced in this study or our previous studies (Appendix 1 Table 1, https://wwwnc.cdc.gov/EID/article/31/1/24-1426-App1.pdf). The best-fit model was selected by ModelFinder (*34*). The trees were visualized with Microreact (https://microreact.org) and adjusted by using the InkScape software (https://www.inkscape.org). ST, sequence type.

carried a *fec* cluster with 100% nt identity and 100% coverage compared with that of *K. pneumoniae* PL3 (Appendix 5 Table, https://wwwnc.cdc.gov/EID/article/31/1/24-1426-App5.xlsx). The *fec* gene cluster was unevenly spread among the 15 most prevalent STs. The *fec* gene cluster was carried by a majority (>50%) of ST258, ST14, ST45, and ST512 isolates and a minority (<10%) of ST16, ST147, ST23, and ST231 isolates. The *fec* genes were more prevalent in ST512 than in the general *K. pneumoniae* population (68% of *fec*-carrying ST512 genomes vs. 37.87% of *fec*-carrying non-ST512 genomes; p<0.00001 by χ^2 test). Most ST512 genomes carried 1 copy of the bla_{KPC} carbapenemase gene (Figure 5), whereas the co-presence of *fec* and bla_{KPC} was less frequent in other clones such as ST101 and ST307 (Figures 6, 7).

Our data suggest that the risk for developing resistance to FDC may be higher in clones like ST512, which more frequently carry the *fec* gene cluster along with the bla_{KPC} gene. The specific FIB(K) replicon, marking the pKPN plasmid, was detected in 16,325 (58.3%) genomes, of which 2,585 (15.8%) also

carried the *fec* cluster of *K. pneumoniae* PL3 (Appendix 2 Table).

Discussion

In vitro studies on FDC resistance have unveiled that CZA-resistant KPC variants (e.g., KPC-31) and class B metallo-β-lactamases have a role in FDC resistance (*35*). Furthermore, mutational inactivation of CirA and Fiu siderophore receptors has been demonstrated to reduce FDC susceptibility in vitro and in vivo (*36,37*).

With this study, our first hypothesis was to attribute FDC resistance of PL3 to bla_{KPC-31} gene duplication (*38-40*). Subsequently, we noticed that PL3 was unique in carrying the *fec* gene cluster on the pKPN plasmid compared with the other PL strains. Consequently, acquisition of the *fec* genes was considered in analysis of genetic traits suspected to increase FDC MIC of PL3. Interest in the FEC transport system was also corroborated by genomic analysis of other *K. pneumoniae* clinical isolates in our collection, given that isolates showing higher FDC MICs also carried the *fec* gene cluster.

With regard to the simplified *E. coli* K-12 laboratory strain model, we speculate that iron imported via the plasmid-encoded FEC system is sufficient to downregulate the expression of Fiu, CirA, FepA and FhuA iron transporters that also mediate FDC import (*37,41,42*). High intracellular iron levels activate the ferric uptake regulator protein, causing general repression of TonB-dependent transporters (*43*).

A recent study reported correlation of FDC resistance with a *fec* gene cluster, originating from *E. coli*, located on an IncC plasmid in VIM-1–producing Enterobacterales (*44*). Our findings extend that observation, demonstrating the effect of the widely diffused plasmid-mediated *fec* gene cluster in globally spread *K. pneumoniae* KPC-carbapenemase producers. In our model, the combination of 2 plasmids (e.g., pKPN and pKpQIL) resulted in reduced susceptibility to FDC. pKpQIL is one of the most diffused plasmids carrying *bla*$_{KPC}$ gene variants. pKPN is a plasmid that seems to be restricted to *K. pneumoniae* and was initially recognized as a vehicle of the *fec* gene cluster in ST307 (*30*).

We show that the *fec* gene cluster is present in many *K. pneumoniae* strains, including those isolated before introduction of FDC in clinical therapy.

Our most relevant evidence is that FDC resistance can be driven by genetic determinants located on plasmids, the success and spread of which occurred independently from the introduction of FDC for therapy. In the future, FDC may act as a positive selector for plasmids carrying the *fec* genes, for which prevalence can be expected to increase.

The results obtained in the *E. coli* experimental model should not allow extrapolation or prediction about the clinical efficacy of FDC in treating infections sustained by *fec*-positive *K. pneumoniae*. However, our study sets the background for future clinical studies aimed at testing the therapeutic efficacy of FDC in infections caused by *K. pneumoniae* carrying different combinations of plasmid-encoded carbapenemases and iron-uptake systems.

During infection, bacteria are faced with the low iron availability imposed by the iron-withholding

Figure 7. Phylogenetic analysis based on core-genome alignments of 1,516 *Klebsiella pneumoniae* ST307 isolates in a study of cefiderocol resistance conferred by plasmid-located ferric citrate transport system in *K. pneumoniae* carbapenemase–producing *K. pneumoniae*. The trees are midpoint rooted, and the scale bar represents the number of substitutions per site. The presence of the *fec* operon is indicated in red; *bla*$_{KPC}$, *bla*$_{VIM}$, and *bla*$_{NDM}$ genes in black; and the FIB(K) replicon in orange. Yellow shading indicates genomes sequenced in this study or our previous studies (Appendix 1 Table 1, https://wwwnc.cdc.gov/EID/article/31/1/24-1426-App1.pdf). The best-fit model was selected by ModelFinder (http://www.iqtree.org/ModelFinder). The trees were visualized with Microreact (https://microreact.org) and adjusted by using the InkScape software (https://www.inkscape.org). ST, sequence type.

aresponse of the host (45) and must therefore express their iron uptake systems for successful tissue invasion and systemic spread (46). Citrate concentrations in biological fluids (≈100 μM in blood) (47) are high enough to activate the *fec* gene cluster; accordingly, selective expression of the FEC system has been documented to contribute to in vivo fitness of *E. coli* in human and animal infection (48–50). Moreover, the introduction of the CZA combination has contributed to selecting *K. pneumoniae* clinical strains that produce CZA-resistant KPC variants, such as KPC-31, characterized by very efficient cephalosporinase activity on the cephalosporin moiety of FDC (38).

Our novel finding is that the combination of a CZA-resistant KPC variant with the FEC system in *K. pneumoniae* may substantially increase the FDC MICs. Thus, the Trojan horse approach is a smart and effective strategy for delivering an antimicrobial drug to its target(s), but *K. pneumoniae* is equipped with plasmids that could help escape that trap.

About the Author

Dr. Polani is a PhD student in the Life Science PhD School of Sapienza University of Rome, Italy. His main interests are genomics of *K. pneumoniae* clones and tracing the evolution of mobile genetic elements involved in the spread of antibiotic resistance genes, particularly those conferring resistance to new antibiotics.

References

1. Miller WR, Arias CA. ESKAPE pathogens: antimicrobial resistance, epidemiology, clinical impact and therapeutics. Nat Rev Microbiol. 2024;22:598–616. https://doi.org/10.1038/s41579-024-01054-w
2. World Health Organization. WHO bacterial priority pathogens list, 2024: bacterial pathogens of public health importance to guide research, development and strategies to prevent and control antimicrobial resistance [cited 2024 Nov 27]. https://www.who.int/publications/i/item/9789240093461
3. Tamma PD, Han JH, Rock C, Harris AD, Lautenbach E, Hsu AJ, et al.; Antibacterial Resistance Leadership Group. Carbapenem therapy is associated with improved survival compared with piperacillin-tazobactam for patients with extended-spectrum β-lactamase bacteremia. Clin Infect Dis. 2015;60:1319–25. https://doi.org/10.1093/cid/civ003
4. Pitout JD, Nordmann P, Poirel L. Carbapenemase-producing *Klebsiella pneum*oniae, a key pathogen set for global nosocomial dominance. Antimicrob Agents Chemother. 2015;59:5873–84. https://doi.org/10.1128/AAC.01019-15
5. Yigit H, Queenan AM, Anderson GJ, Domenech-Sanchez A, Biddle JW, Steward CD, et al. Novel carbapenem-hydrolyzing beta-lactamase, KPC-1, from a carbapenem-resistant strain of *Klebsiella pneumoniae.* Antimicrob Agents Chemother. 2001;45:1151–61. https://doi.org/10.1128/AAC.45.4.1151-1161.2001
6. Chen L, Mathema B, Chavda KD, DeLeo FR, Bonomo RA, Kreiswirth BN. Carbapenemase-producing *Klebsiella pneumoniae*: molecular and genetic decoding. Trends Microbiol. 2014;22:686–96. https://doi.org/10.1016/j.tim.2014.09.003
7. Leavitt A, Chmelnitsky I, Ofek I, Carmeli Y, Navon-Venezia S. Plasmid pKpQIL encoding KPC-3 and TEM-1 confers

carbapenem resistance in an extremely drug-resistant epidemic *Klebsiella pneumoniae* strain. J Antimicrob Chemother. 2010;65:243–8. https://doi.org/10.1093/jac/dkp417

8. Shirley M. Ceftazidime-avibactam: a review in the treatment of serious gram-negative bacterial infections. Drugs. 2018;78:675–92. https://doi.org/10.1007/s40265-018-0902-x

9. Yahav D, Giske CG, Grāmatniece A, Abodakpi H, Tam VH, Leibovici L. New β-lactam-β-lactamase inhibitor combinations. Clin Microbiol Rev. 2020;34:e00115–20. https://doi.org/10.1128/CMR.00115-20

10. Shields RK, Chen L, Cheng S, Chavda KD, Press EG, Snyder A, et al. Emergence of ceftazidime-avibactam resistance due to plasmid-borne bla_{KPC-3} mutations during treatment of carbapenem-resistant *Klebsiella pneumoniae* infections. Antimicrob Agents Chemother. 2017;61:e02097–16.

11. Humphries RM, Yang S, Hemarajata P, Ward KW, Hindler JA, Miller SA, et al. First report of ceftazidime-avibactam resistance in a KPC-3-expressing *Klebsiella pneumoniae* isolate. Antimicrob Agents Chemother. 2015;59:6605–7. https://doi.org/10.1128/AAC.01165-15

12. Hobson CA, Pierrat G, Tenaillon O, Bonacorsi S, Bercot B, Jaouen E, et al. *Klebsiella pneumoniae* carbapenemase variants resistant to ceftazidime-avibactam: an evolutionary overview. Antimicrob Agents Chemother. 2022;66:e0044722. https://doi.org/10.1128/aac.00447-22

13. Taracila MA, Bethel CR, Hujer AM, Papp-Wallace KM, Barnes MD, Rutter JD, et al. Different conformations revealed by NMR underlie resistance to ceftazidime/avibactam and susceptibility to meropenem and imipenem among D179Y variants of KPC β-lactamase. Antimicrob Agents Chemother. 2022;66:e0212421. https://doi.org/10.1128/aac.02124-21

14. Sato T, Yamawaki K. Cefiderocol: discovery, chemistry, and in vivo profiles of a novel siderophore cephalosporin. Clin Infect Dis. 2019;69(Suppl 7):S538–43. https://doi.org/10.1093/cid/ciz826

15. Wu JY, Srinivas P, Pogue JM. Cefiderocol: a novel agent for the management of multidrug-resistant gram-negative organisms. Infect Dis Ther. 2020;9:17–40. https://doi.org/10.1007/s40121-020-00286-6

16. Bolger AM, Lohse M, Usadel B. Trimmomatic: a flexible trimmer for Illumina sequence data. Bioinformatics. 2014;30:2114–20. https://doi.org/10.1093/bioinformatics/btu170

17. Bankevich A, Nurk S, Antipov D, Gurevich AA, Dvorkin M, Kulikov AS, et al. SPAdes: a new genome assembly algorithm and its applications to single-cell sequencing. J Comput Biol. 2012;19:455–77. https://doi.org/10.1089/cmb.2012.0021

18. Freire B, Ladra S, Parama JR. Memory-efficient assembly using Flye. IEEE/ACM Trans Comput Biol Bioinform. 2022;19:3564–77. https://doi.org/10.1109/TCBB.2021.3108843

19. Wick RR, Judd LM, Gorrie CL, Holt KE. Unicycler: resolving bacterial genome assemblies from short and long sequencing reads. PLOS Comput Biol. 2017;13:e1005595. https://doi.org/10.1371/journal.pcbi.1005595

20. Bouras G, Houtak G, Wick RR, Mallawaarachchi V, Roach MJ, Papudeshi B, et al. Hybracter: enabling scalable, automated, complete and accurate bacterial genome assemblies. Microb Genom. 2024;10:001244. https://doi.org/10.1099/mgen.0.001244

21. Seemann T. Prokka: rapid prokaryotic genome annotation. Bioinformatics. 2014;30:2068–9. https://doi.org/10.1093/bioinformatics/btu153

22. von Gabain A, Belasco JG, Schottel JL, Chang AC, Cohen SN. Decay of mRNA in *Escherichia coli*: investigation of the fate of specific segments of transcripts. Proc Natl Acad Sci U S A. 1983;80:653–7. https://doi.org/10.1073/pnas.80.3.653

23. Trirocco R, Pasqua M, Tramonti A, Grossi M, Colonna B, Paiardini A, et al. Fatty acids abolish *Shigella* virulence by inhibiting its master regulator, VirF. Microbiol Spectr. 2023;11:e0077823. https://doi.org/10.1128/spectrum.00778-23

24. Page AJ, Cummins CA, Hunt M, Wong VK, Reuter S, Holden MT, et al. Roary: rapid large-scale prokaryote pan genome analysis. Bioinformatics. 2015;31:3691–3. https://doi.org/10.1093/bioinformatics/btv421

25. Katoh K, Misawa K, Kuma K, Miyata T. MAFFT: a novel method for rapid multiple sequence alignment based on fast Fourier transform. Nucleic Acids Res. 2002;30:3059–66. https://doi.org/10.1093/nar/gkf436

26. Minh BQ, Schmidt HA, Chernomor O, Schrempf D, Woodhams MD, von Haeseler A, et al. IQ-TREE 2: new models and efficient methods for phylogenetic inference in the genomic era. Mol Biol Evol. 2020;37:1530–4. https://doi.org/10.1093/molbev/msaa015

27. Carattoli A, Arcari G, Bibbolino G, Sacco F, Tomolillo D, Di Lella FM, et al. Evolutionary trajectories toward ceftazidime-avibactam resistance in *Klebsiella pneumoniae* clinical isolates. Antimicrob Agents Chemother. 2021;65:e0057421. https://doi.org/10.1128/AAC.00574-21

28. Arcari G, Cecilia F, Oliva A, Polani R, Raponi G, Sacco F, et al. Genotypic evolution of *Klebsiella pneumoniae* sequence type 512 during ceftazidime/avibactam, meropenem/vaborbactam, and cefiderocol treatment, Italy. Emerg Infect Dis. 2023;29:2266–74. https://doi.org/10.3201/eid2911.230921

29. Braun V, Hartmann MD, Hantke K. Transcription regulation of iron carrier transport genes by ECF sigma factors through signaling from the cell surface into the cytoplasm. FEMS Microbiol Rev. 2022;46:fuac010. https://doi.org/10.1093/femsre/fuac010

30. Villa L, Feudi C, Fortini D, Brisse S, Passet V, Bonura C, et al. Diversity, virulence, and antimicrobial resistance of the KPC-producing *Klebsiella pneumoniae* ST307 clone. Microb Genom. 2017;3:e000110. https://doi.org/10.1099/mgen.0.000110

31. Livak KJ, Schmittgen TD. Analysis of relative gene expression data using real-time quantitative PCR and the $2^{-\Delta\Delta CT}$ method. Methods. 2001;25:402–8. https://doi.org/10.1006/meth.2001.1262

32 Enz S, Mahren S, Menzel C, Braun V. Analysis of the ferric citrate transport gene promoter of *Escherichia coli*. J Bacteriol. 2003;185:2387–91. https://doi.org/10.1128/JB.185.7.2387-2391.2003

33. Angerer A, Braun V. Iron regulates transcription of the *Escherichia coli* ferric citrate transport genes directly and through the transcription initiation proteins. Arch Microbiol. 1998;169:483–90. https://doi.org/10.1007/s002030050600

34. Kalyaanamoorthy S, Minh BQ, Wong TKF, von Haeseler A, Jermiin LS. ModelFinder: fast model selection for accurate phylogenetic estimates. Nat Methods. 2017;14:587–9. https://doi.org/10.1038/nmeth.4285

35. Simner PJ, Bergman Y, Conzemius R, Jacobs E, Tekle T, Beisken S, et al. An NDM-producing *Escherichia coli* clinical isolate exhibiting resistance to cefiderocol and the combination of ceftazidime-avibactam and aztreonam: another step toward pan-β-lactam resistance. Open Forum Infect Dis. 2023;10:ofad276. https://doi.org/10.1093/ofid/ofad276

36. McElheny CL, Fowler EL, Iovleva A, Shields RK, Doi Y. *In vitro* evolution of cefiderocol resistance in an NDM-producing *Klebsiella pneumoniae* due to functional loss of

CirA. Microbiol Spectr. 2021;9:e0177921. https://doi.org/10.1128/Spectrum.01779-21

37. Lan P, Lu Y, Jiang Y, Wu X, Yu Y, Zhou J. Catecholate siderophore receptor CirA impacts cefiderocol susceptibility in *Klebsiella pneumoniae.* Int J Antimicrob Agents. 2022;60:106646. https://doi.org/10.1016/j.ijantimicag.2022.106646

38. Poirel L, Sadek M, Kusaksizoglu A, Nordmann P. Co-resistance to ceftazidime-avibactam and cefiderocol in clinical isolates producing KPC variants. Eur J Clin Microbiol Infect Dis. 2022;41:677–80. https://doi.org/10.1007/s10096-021-04397-x

39. Coppi M, Di Pilato V, Monaco F, Giani T, Conaldi PG, Rossolini GM. Ceftazidime-avibactam resistance associated with increased bla_{KPC-3} gene copy number mediated by pKpQIL plasmid derivatives in sequence type 258 *Klebsiella pneumoniae.* Antimicrob Agents Chemother. 2020;64:e01816–9. https://doi.org/10.1128/AAC.01816-19

40. Hobson CA, Cointe A, Jacquier H, Choudhury A, Magnan M, Courroux C, et al. Cross-resistance to cefiderocol and ceftazidime-avibactam in KPC β-lactamase mutants and the inoculum effect. Clin Microbiol Infect. 2021;27:1172. e7–10. https://doi.org/10.1016/j.cmi.2021.04.016

41. Pressler U, Staudenmaier H, Zimmermann L, Braun V. Genetics of the iron dicitrate transport system of *Escherichia coli.* J Bacteriol. 1988;170:2716–24. https://doi.org/10.1128/jb.170.6.2716-2724.1988

42. Staudenmaier H, Van Hove B, Yaraghi Z, Braun V. Nucleotide sequences of the *fecBCDE* genes and locations of the proteins suggest a periplasmic-binding-protein-dependent transport mechanism for iron(III) dicitrate in *Escherichia coli.* J Bacteriol. 1989;171:2626–33. https://doi.org/10.1128/jb.171.5.2626-2633.1989

43. Baichoo N, Helmann JD. Recognition of DNA by Fur: a reinterpretation of the Fur box consensus sequence. J Bacteriol. 2002;184:5826–32. https://doi.org/10.1128/JB.184.21.5826-5832.2002

44. Kocer K, Boutin S, Heeg K, Nurjadi D. The acquisition of transferable extrachromosomal *fec* operon is associated with a cefiderocol MIC increase in Enterobacterales. J Antimicrob Chemother. 2022;77:3487–95. https://doi.org/10.1093/jac/dkac347

45. Ganz T, Nemeth E. Iron homeostasis in host defence and inflammation. Nat Rev Immunol. 2015;15:500–10. https://doi.org/10.1038/nri3863

46. Page MGP. The role of iron and siderophores in infection, and the development of siderophore antibiotics. Clin Infect Dis. 2019;69(Suppl 7):S529–37. https://doi.org/10.1093/cid/ciz825

47. Costello LC, Franklin RB. Plasma citrate homeostasis: how it is regulated; and its physiological and clinical implications. an important, but neglected, relationship in medicine. HSOA J Hum Endocrinol. 2016;1:005.

48. Frick-Cheng AE, Sintsova A, Smith SN, Pirani A, Snitkin ES, Mobley HLT. Ferric citrate uptake is a virulence factor in uropathogenic *Escherichia coli.* MBio. 2022;13:e0103522. https://doi.org/10.1128/mbio.01035-22

49. Huang WC, Wong MY, Wang SH, Hashimoto M, Lin MH, Lee MF, et al. The ferric citrate uptake system encoded in a novel $bla_{CTX-M-3}$- and bla_{TEM-1}-harboring conjugative plasmid contributes to the virulence of *Escherichia coli.* Front Microbiol. 2021;12:667782. https://doi.org/10.3389/fmicb.2021.667782

50. Blum SE, Goldstone RJ, Connolly JPR, Répérant-Ferter M, Germon P, Inglis NF, et al. Postgenomics characterization of an essential genetic determinant of mammary pathogenic *Escherichia coli.* MBio. 2018;9:e00423–18. https://doi.org/10.1128/mBio.00423-18

Address for correspondence: Alessandra Carattoli, Department of Molecular Medicine, Sapienza University of Rome, Viale Porta Tiburtina 28, 00185 Rome, Italy; email: alessandra.carattoli@uniroma1.it